Scripta METALLURGICA Vol. 22, pp. 1547-1551, 1988 Pergamon Press plc
Printed in the U.S.A.

ON MISFIT-INDUCED LATTICE SPACING VARIATIONS IN TWO-PHASE ALLOYS: THE CASE OF COOLING-INDUCED MICROSTRAINS IN THE Al-MATRIX OF FULLY AGED AlSi ALLOYS

P. van Mourik, Th.H. de Keijser, N.M. van der Pers, E.J. Mittemeijer

Laboratory of Metallurgy, Delft University of Technology,
Rotterdamseweg 137, 2628 AL Delft,The Netherlands

(Received June 20, 1988)

1.Introduction

On the ageing of supersaturated solid solutions, elastic strains develop as a result of the volume misfit between the precipitating disperse (non-equilibrium) phase(s) and the, continuous, matrix phase. This is the basis of the well known, but not fully understood, precipitation hardening of alloys. Knowledge of the development of internal strain distributions may be of great use for the understanding of the macroscopic mechanical properties of multiphase materials.

Consider a specimen composed of a matrix A and homogeneously distributed particles B. Elastic strains in such an assembly occur if the B-particles do not fit without deformation into the holes provided by the A-matrix. The origin of such a misfit can be various, e.g. atomic volume changes caused by precipitation of the B-particles or differences in shrinkage between the A-matrix and the B-particles on cooling after a heat treatment.

From an experimental point of view, one can distinguish macro- and microstrains. By definition, a macrostrain is related to the *average* lattice spacing of a phase, whereas a microstrain corresponds to an average of the variations in the lattice spacing. Therefore, both macro- and microstrains can be detected by X-ray diffraction: macrostrains cause shifts of the diffraction lines and microstrains induce broadening of the diffraction lines.

The occurrence of *macrostrains* in a matrix containing misfitting second phase particles was investigated earlier (1,2). On the basis of a theory developed by Eshelby (3) for the elastic strains in a continuous isotropic matrix due to misfitting inclusions and originally applied to crystals containing point imperfections, a relation was derived (see Section 2) between the macrostrain, the volume fraction y_B of B-particles, a misfit parameter ε and a constant C_A reflecting the elastic properties of both the matrix and the inclusions (1,4). In the case of point imperfections the theory has its limitations (5). However, these may be less significant for inclusions composed of a number of atoms.

An experimental test was performed on two-phase AlSi and FeN alloys. Because precipitation stresses due to differences in molar volume were completely relaxed in the fully aged AlSi alloys (Al-matrix + Si-particles) (1,4), the misfit solely stemmed from the difference in shrinkage between the Al-matrix and the precipitated Si-particles on cooling from the ageing temperature T_a to room temperature T_r and the misfit parameter ε could be quantified easily (see Section 4). A fair agreement between theory and experiment was established (1). A very good agreement between theory and experiment was obtained for the fully aged two-phase FeN alloys (α-Fe matrix + α''-$Fe_{16}N_2$ particles), where the misfit was solely due to differences in molar volume (2).

To our knowledge a quantitative interpretation of *microstrains*, i.e. of diffraction line broadening, in a matrix containing misfitting particles has not been given before. The aim of the present study is to describe the microstrain quantitatively and to perform an experimental test on fully aged AlSi alloys.

2. Theory

In Eshelby's theory the distinction between an infinite and a finite A-matrix is essential.

Inserting a misfitting spherical B-particle into a cavity of an *infinite*, continuous and isotropic A-matrix causes stresses in all directions. Taking the origin in the centre of the B-particle and considering only the displacements in the A-matrix it can be shown that, in polar coordinates (r,φ,θ), the mutually perpendicular local strain components are given by (5):

$$e_{rr} = -2\,C\,\varepsilon\,(r_o^A)^3/r^3\,; \qquad e_{\varphi\varphi} = e_{\theta\theta} = C\,\varepsilon(r_o^A)^3/r^3 \qquad (r > r_o^A) \qquad [1]$$

0036-9748/88 $3.00 + .00

where $C = 3K_B/(3K_B + 4\mu_A)$ with μ and K denoting the shear and the bulk modulii and where - with r_o^A and r_o^B as the radii of the undeformed cavity in the A-matrix and of the undeformed B-particle - the misfit parameter ε is given by: $\varepsilon = (r_o^B - r_o^A)/r_o^A$. The B-particle is only subjected to a uniform hydrostatic stress, implying the absence of microstrains. As the relative volume change of the matrix $\Delta V_A/V_A$ equals $e_{rr} + e_{\varphi\varphi} + e_{\theta\theta}$, it follows directly from eq. [1] that for an infinite A-matrix no volume change, and therefore no macrostrain, occurs at all on inserting a misfitting B-particle. Hence, the stress components for the A-matrix can be written in terms of the shear modulus μ_A:

$$X_{rr} = -4\mu_A C \varepsilon (r_o^A)^3/r^3; \qquad X_{\varphi\varphi} = X_{\theta\theta} = 2\mu_A C \varepsilon (r_o^A)^3/r^3 \qquad (r > r_o^A) \qquad [2]$$

A *finite* spherical assembly of an A-matrix with a spherical B-particle has a traction-free bounding surface. To fulfil this requirement, the stress along the radius vector $\underline{r}$ has to be compensated by a hydrostatic stress equal to $-X_{rr}$ (r = R) where R is the radius of the assembly. This hydrostatic stress changes the volume of the matrix (1,4) and therefore macrostresses occur in a *finite* matrix. For a cubic matrix with lattice parameter a_A the macrostrain $e_u = \Delta a_A/a_A$ follows, via $\Delta V_A/V_A = 3\Delta a_A/a_A = -X_{rr}$ (r = R)/K_A, from eq. [2]:

$$e_u = 4 C_A \varepsilon (r_o^A)^3/R^3 = 4 C_A \frac{\varepsilon}{(1+\varepsilon)^3} y_B \qquad [3]$$

where $C_A = C\mu_A/3K_A$ and y_B is the volume fraction of B. Equation [3] also holds for a matrix containing a number of B-particles whose strain fields are independent.

The strain e_u is uniform throughout the finite matrix and therefore does not contribute to the broadening of matrix reflections.The breadth of an X-ray diffraction line is connected with $\langle e^2 \rangle$, i.e. the volume average of the square of the position-dependent part of the strain in the direction perpendicular to the diffracting planes (hkl) (6). For an elastically isotropic matrix in which the strain field has spherical symmetry it holds that (i) $\langle e^2 \rangle$ is the same for all (hkl) and (ii) the average over a sphere of radius r around the origin of the squared position-dependent strains perpendicular to the diffracting planes, $\langle e^2(r) \rangle$, is equal to the average over all directions (φ,θ) of the squared strains at a point (r,φ,θ). Then it follows:

$$\langle e^2(r) \rangle = \frac{1}{5}(e_{rr}^2 + e_{\varphi\varphi}^2 + e_{\theta\theta}^2) + \frac{2}{15}(e_{rr}e_{\varphi\varphi} + e_{rr}e_{\theta\theta} + e_{\varphi\varphi}e_{\theta\theta}) \qquad [4]$$

Substitution of eq. [1] yields:

$$\langle e^2(r) \rangle = \frac{4}{5} C^2 \varepsilon^2 (r_o^A)^6/r^6 \qquad [5]$$

By averaging over the total volume, i.e. over all distances $r^B \leq r \leq R$, one obtains (see also eq. [3]):

$$\langle e^2 \rangle = \frac{4}{5} C^2 \frac{\varepsilon^2}{(1+\varepsilon)^6} y_B \qquad [6]$$

Eq.[6] also holds for a matrix containing a number of B-particles, whose strain fields in the matrix are independent (see eq. [3]).

This result can also be obtained in an indirect way from the energy E_A, associated with the strain field in an infinite matrix (no uniform strain). From eqs. [1] and [2] it is obtained (cf. Ref. 5):

$$E_A = 6\mu_A C^2 \frac{\varepsilon^2}{(1+\varepsilon)^6} y_B \qquad [7]$$

According to the reasoning by Faulkner (7), it follows for the present symmetry:

$$E_A = \frac{15}{2} \mu_A \langle e^2 \rangle \qquad [8]$$

From eqs. [7] and [8], eq. [6] follows directly.

The integral breadth of a strain-broadened line profile, i.e. integral intensity divided by maximum intensity, is related to the microstrain $\langle e^2 \rangle^{1/2}$ by:

$$\langle e^2 \rangle^{1/2} = k \beta \cot \theta_B \qquad [9]$$

where θ_B is Bragg's angle and k is a proportionality constant, which, as usual, is taken here as 1/4 (6).

3. Experimental Procedures

Ribbons (thickness 20-50 mm) of AlSi alloys with 0, 2.3, 4.2, 5.9, 11.9 and 18.2 at% Si were prepared by meltspinning from 99.998 wt% Al and 99.99 wt% Si (8). According to dendrite arm spacing measurements the cooling rate was in the range of 10^6 - 10^7 Ks^{-1}. To be sure of a completed silicon precipitation ((9);see also Section 4), sections of the ribbons were (fully) aged during 1841 h at 447 ± 2 K in an oil bath and cooled in air. The preparation of specimens for X-ray diffractometry consisted of placing pieces of ribbon parallel to each other on a flat plastic turntable with the aid of adhesive tape, alternating up- and wheelsides. So, the data obtained are averages for the up- and wheelsides (10).

The X-ray diffraction line profiles were chosen on the following grounds: (i) high $2\theta_B$ reflections to improve accuracy, (ii) different crystallographic directions to investigate effects due to a possible lack of isotropy, and (iii) minimal disturbance by neighbouring diffraction lines from Si-particles. The Al{400}-, Al{331}- and Al{420}-line profiles were selected; only the Si{531}-reflection was situated between the Al{331}- and the Al{420}-line profiles. The profiles were recorded using a Siemens ω-diffractometer employing CuKα-radiation (45 kV, 25 mA). The profiles were measured by the preset-time method with steps of 0.02°2θ. Large portions of the background at both sides of the peak were recorded.

To remove the so-called instrumental broadening and the broadening due to the X-ray wavelength distribution the corresponding line profiles of co-aged pure aluminium ribbons served as references (10). The background was linearly interpolated between the extremities of the profile measured. The analysis of the line profiles was performed by the so-called single-line Voigt method, assuming that both the reference profile and the line profile to be analysed could be described by a Voigt-function (11). As the recorded profiles were relatively sharp, no corrections for the angle dependence of the Lorentz-polarisation and the absorption factors were considered to be necessary. Before applying the single-line Voigt method, the α_2-components of the profiles were eliminated.

In practice it is often considered that a finite crystallite size results in Cauchy-shaped profiles and that microstrains result in Gaussian-shaped profiles (11). In the present case, it appeared that the Al-matrix line profiles corrected for instrumental effects were almost entirely of Gaussian shape. Therefore, the structural line broadening of the Al-matrix line profiles investigated was interpreted as only caused by microstrains.

For the presence of overlapping tails of the Si{531} reflection the following correction procedure was applied to the Al{331} and Al{420} profiles. For the alloy with the highest silicon content the overlapping Si{531} tails were eliminated by an educated guess, which gave an increase of 10% of the microstrain as compared to the microstrain obtained without elimination. Then for the remaining alloys the microstrain values obtained from the Al{331} and Al{420} reflections, without elimination of the overlapping Si{531} tails, were increased in proportion to the silicon content of the alloy concerned.

4. Results and Discussion

In fully aged AlSi alloys, consisting of an Al-matrix and dispersed Si-particles, a contribution to the broadening of the Al-matrix line profiles can be expected from (i) composition variations in the Al-matrix, (ii) lattice defects as dislocations, and (iii) misfit phenomena. Composition variations in decomposing alloys would generally result in asymmetrical Al-matrix line profiles (12). However, the observed Al-matrix profiles are symmetrical. Further, at the ageing temperature applied the silicon equilibrium solubility in the Al-matrix is negligible (13). So, it is concluded that cause (i) does not contribute to the line broadening observed. A substantial density of lattice defects as dislocations in the Al-matrix is not expected since the motion of dislocations is not much obstructed in the matrix of almost pure Al at the relatively high ageing temperature applied: 447 ± 2 K, which is almost half the melting point of Al. Further, one should expect about the

same lattice defect density in the pure Al reference specimen (see Section 3) and by the line profile analysis technique applied here (relative determinations, see Ref. 14), a possible presence of lattice defects is not reflected in the values for the microstrains obtained.

Misfit phenomena can be caused by:

a. the difference in atomic volume between silicon dissolved and silicon precipitated;
b. the difference in thermal shrinkage between the Al-matrix and the Si-particles on cooling from the ageing temperature T_a to room temperature T_r.

The difference in atomic volume causes strains during silicon precipitation (4,9), that relax during and after precipitation (15). At about 450 K this process of silicon precipitation and stress relaxation in melt-spun AlSi alloys has been completed after 32 h of ageing (4,9). The applied ageing treatment in this investigation was 1841 h at 447 ± 2 K. So, the only origin of Al-matrix line broadening is the difference in thermal shrinkage between the Si-particles and the surrounding Al-matrix.

The misfit parameter ε then reads (1):

$$\varepsilon = (\alpha_{Al} - \alpha_{Si})(T_a - T_r) = \Delta\alpha\Delta T \qquad [10]$$

where α_{Al} and α_{Si} are the thermal linear expansion coefficients of the Al-matrix and the Si-particles.

The fully aged melt-spun AlSi alloys can be regarded as a model system for the study of the elastic effects due to the presence of misfitting second phase particles since:

(i) the large difference in thermal expansion coefficients of the Al-matrix and the Si-particles ($\Delta\alpha = 20.5 \times 10^{-6}\ K^{-1}$ (4)) yields a large misfit parameter.
(ii) the Al-matrix can be regarded as elastically isotropic (16).
(iii) the Si-particles in melt-spun AlSi alloys can be considered as small spheres (1).

In Fig. 1 the theoretical and experimental values of $\langle e^2\rangle^{1/2}/\Delta T$ as obtained for the fully aged melt-spun AlSi alloys from the different Al-matrix reflections are plotted as a function of $(y_{Si})^{1/2}$ (The volume fraction y_{Si} was calculated from the overall composition of the alloy concerned; the value of C in eqs. [1] and [6] was obtained from the elastic constants of the elements (16), giving a theoretical value of $C^{th} = 0.73$). For the ageing temperature applied the value of $(1 + \varepsilon)$ can be put equal to one. As prescribed by eq. [6], the experimental data lie on a straight line through the origin, the slope of which is only slightly different from the predicted value. As a function of y_{Si} (the alloy composition) no distinct differences occur between the values of $\langle e^2\rangle^{1/2}/\Delta T$ obtained from the different Al-matrix line profiles {400}, {331} and {420}. This justifies the assumption of elastic isotropy.

The value for C in eqs. [1] and [6] as deduced from the straight line through the experimental data in Fig. 1 equals $C^{exp} = 0.67$ which is about 10% smaller than $C^{th} = 0.73$. The proportionality constant C_A in eq. [3] for the *macrostrain* as deduced from experiments was about 30% larger than the one calculated from literature data: $C_A^{exp} = 0.112$ to compare with $C_A^{th} = 0.086$ (4).

Considering the simplicity of the model applied, the compatibility of the used literature data for the elastic constants with the model and the uncertainties in the line profile analyses, e.g. about the value of k in eq. [9], a satisfactory correspondence occurs between theory and experiment, not only for the *macrostrain* (1,2), but also for the *microstrain* (present work).

Acknowledgement

Dr.Ir. R. Delhez made available to us computer software to perform the single-line Voigt analysis.

References

1. E.J. Mittemeijer, P. van Mourik, Th.H. de Keijser, Phil. Mag. A, A42, 1157 (1981).
2. E.J. Mittemeijer, A. van Gent, Scripta Met. 18, 825 (1984).
3.a. J.D. Eshelby, J. Appl. Phys. 25, 255 (1954).
3.b. J.D. Eshelby, Solid State Phys. 3, 79 (1956).
4. P. van Mourik, Th.H. de Keijser, E.J. Mittemeijer, in "Rapidly Solidified Materials", Conference Proceedings ed. by P.W. Lee and R.S. Carbonara, p. 342, ASM, Metals Park, Ohio (USA) (1986).
5. J.W. Christian, "The Theory of Transformations in Metals and Alloys", part I, 2nd edn., p. 198, Pergamon Press, Oxford (1978).
6. R. Delhez, Th.H. de Keijser, E.J. Mittemeijer, Fresenius Z. Anal. Chem. 312, 1 (1982).

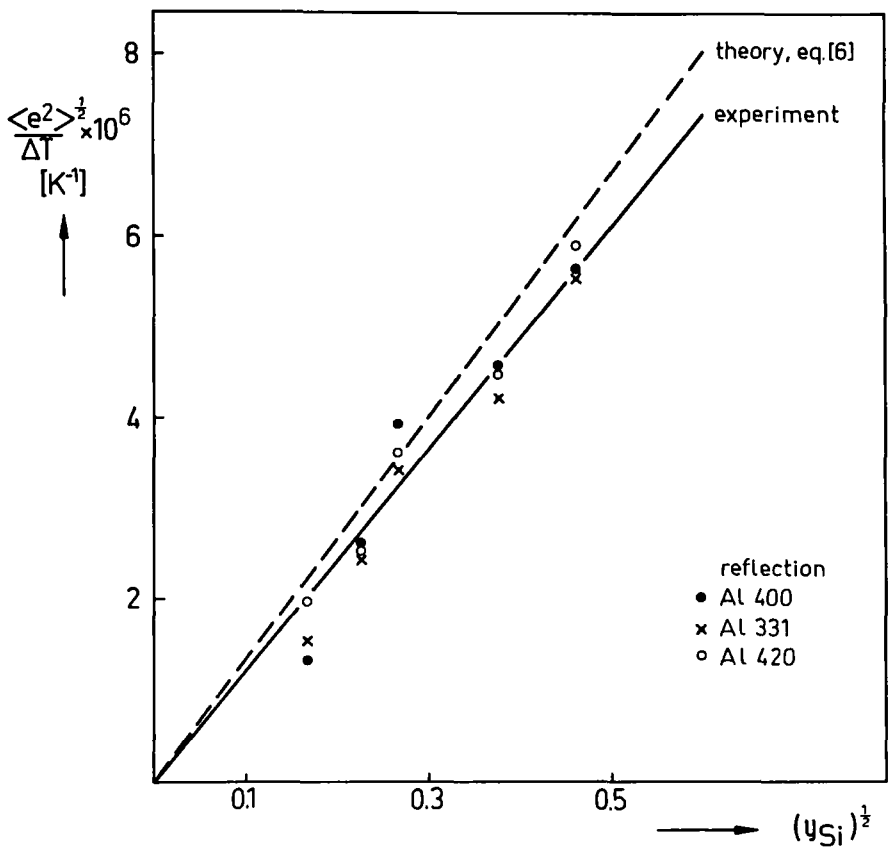

FIGURE 1- The microstrain in the Al-matrix of fully aged AlSi alloys per Kelvin difference between ageing and room temperature, $\langle e^2\rangle^{1/2}/\Delta T$, as a function of the square root of the volume fraction of Si-phase, $(y_{Si})^{1/2}$.

7. E.A. Faulkner, Phil. Mag. 5, 519 (1960).
8. A. Bendijk, R. Delhez, L. Katgerman, E.J. Mittemeijer, N.M. van der Pers, J. of Mat Sci. 15, 2803 (1980).
9. P. van Mourik, E.J. Mittemeijer, Th.H. de Keijser, J. of Mat. Sci. 18, 2706 (1983).
10. R. Delhez, Th.H. de Keijser, E.J. Mittemeijer, P. van Mourik, N.M. van der Pers, L. Katgerman, W.E. Zalm, J. of Mat. Sci. 17, 2887 (1982).
11. Th.H. de Keijser, J.I. Langford, E.J. Mittemeijer, A.B.P. Vogels, J. Appl. Cryst. 15, 308 (1982).
12. P. van Mourik, N.M. Maaswinkel, Th.H. de Keijser, E.J. Mittemeijer, in preparation.
13. J.L. Murray, A.J. McAlister, Bull. of Alloy Phase Diagr. 5, 74 (1984).
14. R. Delhez, Th.H. de Keijser, E.J. Mittemeijer, J.I. Langford, Proc. of the Int. Symposium on X-ray Powder Diffractometry, 13-17 August 1987, Fremantle (Australia), Australian J. of Phys. 41 (1988) in the press.
15. P. van Mourik, Th.H. de Keijser, E.J. Mittemeijer, Scripta Met. 21, 381 (1987).
16. C.J. Smithells, "Metals Reference Book", Butterworths, London, 1976.